



The many-body expansion: From hydrogen bonded to light nuclear systems

Demeter Tzeli^{a,b,*} and Sotiris S. Xantheas^{c,d,e,*}

^aLaboratory of Physical Chemistry, Department of Chemistry, National and Kapodistrian University of Athens, Athens, Greece

^bTheoretical and Physical Chemistry Institute, National Hellenic Research Foundation, Athens, Greece

^cAdvanced Computing, Mathematics and Data Division, Pacific Northwest National Laboratory, Richland, Washington, United States

^dPacific Northwest National Laboratory, Computational and Theoretical Chemistry Institute (CTCI), Richland, WA, United States

^eDepartment of Chemistry, University of Washington, Seattle, Washington, United States

*Corresponding authors. e-mail address: tzeli@chem.uoa.gr; dtzeli@cie.gr; sotiris.xantheas@pnnl.gov; xantheas@uw.edu

Contents

1. Introduction	96
2. The MBE formulation	98
3. Breaking covalent bonds: The concept of the in situ electronic state of an atom in a molecule	99
4. Covalently bonded molecules	100
5. Metallic clusters	105
6. Light nuclei	110
7. Conclusions	113
Acknowledgments	115
References	115

Abstract

The Many-Body Expansion (MBE) is based on combinatorial mathematics, and it is commonly used to analyze and understand the composition of interatomic and intermolecular interactions, while in practice it has facilitated the calculations of large aqueous systems. In this chapter, the application of MBE is extended into (a) molecular systems that are formed via covalent bonds, (b) metal clusters and (c) light nuclei. These three categories of systems have distinct characteristics and as such they pose significant challenges compared to the hydrogen bonded ones, where the MBE has been used routinely. In the latter a “body” is a well-defined chemical system (water, ion, solute), no covalent bonds need to be broken to define the various “bodies” used in the expansion, whereas the one-body term corresponds to geometric deformations due to the interactions that are associated with spectral signatures probed by infrared (IR) spectroscopy. In contrast, for cases (a) and (b) contained here, the MBE is carried

out by breaking chemical bonds, i.e., covalent, ionic, metallic or coordination bonds. The one-body is evaluated via the “in situ” electronic structure of the atoms in the various “bodies” (atoms, diatomics, triatomics etc.) as the energy required to promote an atom from its ground state to its in situ electronic state within the fragment. Metallic systems, in addition, present additional challenges due to their complex electronic structure and strong short-range interactions, which are more pronounced than in molecular systems. Accurately describing the multi-coordinated bonding in metals often requires accounting for both static and dynamic electron correlation effects, along with careful treatment of spin multiplicities in intermediate structures involving open-shell metal species. Finally, for (c) light nuclei, the MBE approach assumes that the kinetic energy is represented by the one-body term. Consequently, light nuclear systems are treated using the same protocol that has been successfully and extensively applied to hydrogen-bonded molecular systems, and more recently, to covalent and metal-metal bonds.



1. Introduction

The Many-Body Expansion (MBE) is a concept based on combinatorial mathematics, and it is typically used to determine how many distinct elements are present when combining multiple finite sets.¹ In mathematics, the MBE assists in breaking down complex systems into manageable sub-parts by considering interactions of increasing size. In physics and chemistry, it is used to approximate properties (like energy) of a many-particle system by summing contributions from individual particles, pairs (2-body systems), triads (3-body systems), etc.²⁻⁴ The purpose of the MBE in quantum chemistry is twofold: in analysis, to understand the composition of interatomic and intermolecular interactions, and in practice, to facilitate calculations on large systems.¹⁻⁷

The MBE concept was applied to chemical physics problems for the first time in the 1970s. In this first study, a trimer of water molecules was studied, where the individual water molecules were considered as the “bodies” connected via hydrogen bonds. The analysis allowed to estimate the non-additive three-body term by partitioning the energy of a water trimer.² Since its initial introduction when the many-body expansion framework was formulated in terms of energies associated with distinct, non-overlapping molecular sub-fragments, the MBE has found widespread application in the study of hydrogen-bonded molecular clusters. This approach has been utilized by numerous groups including us²⁻²⁶ to rigorously assess and quantify the contribution of the non-additive energy components to the total binding energies of aqueous clusters.²⁷

More recently, further developments have expanded the scope and utility of the MBE, particularly through the incorporation of high-level electronic structure calculations. These advances have examined how the accuracy of the MBE depends on important computational parameters such as the size of the orbital basis set and the level of electron correlation employed within the expansion.^{28–30} In parallel, a molecular dynamics methodology that integrates the MBE framework (referred to as MBE-MD) has been introduced,³¹ providing dynamic insights into many-body effects in hydrogen-bonded systems and also extended to periodic systems.³² Note that this scheme will not be appropriate for treating metallic clusters as there are several paths incorporating different electronic states to build up the collection of “bodies” in the expansion.

This specific formulation of the MBE—tailored for hydrogen-bonded molecular systems, including ionic species—relies on a clear and intuitive definition of a “body,” wherein the system is partitioned into non-overlapping fragments (e.g., monomers, dimers, trimers, etc.) through the simple process of breaking hydrogen bonds. This methodological approach has made it particularly suitable for the construction of highly accurate, ab initio-based many-body potential energy surfaces for water and related systems.^{33–49} It is important to contrast this approach with alternative partitioning strategies that utilize overlapping sub-fragments, such as those employed in the Molecular Tailoring Approach (MTA),^{50–54} or other general fragmentation-based techniques,^{7,55–58} which often adopt a different philosophy in the fragment definition and recombination. Additionally, the MBE has also been extended beyond spatial fragmentation schemes to energy extrapolation techniques where molecular orbitals themselves are treated as the “bodies” of the expansion. This variant has proven effective in estimating the total electron correlation energy in both molecular systems^{59–64} and crystalline solids.^{65,66}

In this chapter, we will discuss the application of the MBE to chemical systems beyond the “well-behaved” hydrogen bonded ones by extending it (a) to systems involving covalent bond dissociation where the polyatomic molecule is treated as a composite of individual atoms, diatomic, triatomic, and higher-order atomic groupings⁶⁷ (b) to metal clusters^{68–70} and (c) to light nuclei.^{71–73} It is important to emphasize that the application of the MBE approach to covalently bonded systems, particularly to metallic structures, presents significant challenges. These arise from their electronic structure and strong short-range interactions characteristic of such systems. Accurately describing the multi-coordinated bonding in metals often

requires accounting for both dynamic and static (non-dynamic) electron correlation effects, along with careful treatment of spin multiplicities in intermediate structures involving open-shell metal species.⁶⁸



2. The MBE formulation

The binding energy of a cluster of n atoms with respect to the ground atomic state products (ΔE_{atomiz}) can be decomposed^{4,11} in one-body (1-B), two-body (2-B), three-body (3-B), four-body (4-B), etc. n -terms for clusters with up to n atoms, see Eqs. (1)–(6),

$$\begin{aligned}\Delta E_{\text{atomiz}} &= E(123 \dots n) - \sum_{i=1}^n E(X_i^{\text{gs}}) \\ &\approx \Delta E(1 - \text{B}) + \Delta E(2 - \text{B}) \\ &\quad + \Delta E(3 - \text{B}) + \dots + \Delta E(n - \text{B})\end{aligned}\quad (1)$$

$$\Delta E(1 - \text{B}) = \sum_i^n (E(X_i) - E(X_i^{\text{gs}})) \quad (2)$$

$$\Delta E(2 - \text{B}) = \sum_{i < j}^n \Delta^2 E_{ij} \quad (3)$$

$$\Delta^2 E_{ij} = E(X_i X_j) - E(X_i) - E(X_j) \quad (4)$$

$$\Delta E(3 - \text{B}) = \sum_{i < j < k}^n \Delta^3 E_{ijk} \quad (5)$$

$$\Delta^3 E_{ijk} = E(X_i X_j X_k) - E(X_i) - E(X_j) - E(X_k) - \Delta^2 E_{ij} - \Delta^2 E_{ik} - \Delta^2 E_{jk} \quad (6)$$

where $E(X_i)$ is the in situ (ground or excited) atomic state, i.e. the atomic state within the molecule or cluster in equilibrium geometry and $E(X_i^{\text{gs}})$ is the ground atomic state of atom X_i . Thus, if the in situ atomic state is the ground state, then the 1-B term is zero.

The corrected binding energies and the many body terms for basis set superposition error (BSSE)^{74–76} are analytically given in references,^{4,11} and.⁷⁷ Thus, the corresponding BSSE corrected ΔE terms of Eqs. (1)–(6), i.e., $\Delta E'_{\text{atomiz}}$, $\Delta E'(2 - \text{B})$, $\Delta E'(3 - \text{B})$, etc. are given in Eqs. (7)–(12).

$$\Delta E'_{\text{atomiz}} = E_{x_1 x_2 x_3 \dots x_n}^{b_1 b_2 b_3 \dots b_n}(X_i X_j X_k \dots X_n) - \sum_{i=1}^n E_{x_i}^{b_1 b_2 b_3 \dots b_n}(X_i^{\text{gs}}) \quad (7)$$

$$\Delta E'(1 - B) = \Delta E(1 - B) \quad (8)$$

$$\Delta E'(2 - B) = \sum_{i < j}^n \Delta^2 E'_{ij} \quad (9)$$

$$\Delta^2 E'_{ij} = E_{x_1 x_2 x_3 \dots x_n}^{b_1 b_2 b_3 \dots b_n}(X_i X_j) - \left[E_{x_1 x_2 x_3 \dots x_n}^{b_1 b_2 b_3 \dots b_n}(X_i) + E_{x_1 x_2 x_3 \dots x_n}^{b_1 b_2 b_3 \dots b_n}(X_j) \right] \quad (10)$$

$$\Delta E'(3 - B) = \sum_{i < j < k}^n \Delta^3 E'_{ijk} \quad (11)$$

$$\begin{aligned} \Delta^3 E'_{ijk} = & E_{x_1 x_2 x_3 \dots x_n}^{b_1 b_2 b_3 \dots b_n}(X_i X_j X_k) - \left[E_{x_1 x_2 x_3 \dots x_n}^{b_1 b_2 b_3 \dots b_n}(X_i) + E_{x_1 x_2 x_3 \dots x_n}^{b_1 b_2 b_3 \dots b_n}(X_j) \right. \\ & \left. + E_{x_1 x_2 x_3 \dots x_n}^{b_1 b_2 b_3 \dots b_n}(X_k) \right] \\ - & \left[\Delta^2 E_{x_1 x_2 x_3 \dots x_n}^{b_1 b_2 b_3 \dots b_n}(X_i X_j) + \Delta^2 E_{x_1 x_2 x_3 \dots x_n}^{b_1 b_2 b_3 \dots b_n}(X_j X_k) + \Delta^2 E_{x_1 x_2 x_3 \dots x_n}^{b_1 b_2 b_3 \dots b_n}(X_i X_k) \right] \end{aligned} \quad (12)$$

where $E_g^b(F)$ is the energy of fragment F calculated with basis set b of the fragment at the fragment's cluster geometry g .



3. Breaking covalent bonds: The concept of the in situ electronic state of an atom in a molecule

The concept of the in situ electronic state of an atom in a molecule for the breaking the covalent bonds stems from previous work by Heitler,⁷⁸ in which he pointed out that the CH_4 minimum correlates with the $\text{C}(^5\text{S}) + 4\text{H}(^2\text{S})$ asymptote, viz. the Carbon atom is $2s^1 2p^3$ hybridized as shown in Fig. 1. In accordance with this observation, we have recently introduced⁶⁷ a novel extension of the MBE framework to systems involving covalent bond dissociation, thereby broadening its application beyond its traditional use in modeling hydrogen bond breaking. A key feature of this new approach is the concept of the in situ atomic electronic state—where the one-body (1-B) term represents the energy required to promote an atom from its ground state to the electronic state it adopts within the molecule. Higher-order terms correspond to the energies of bonded fragments such as diatomic,

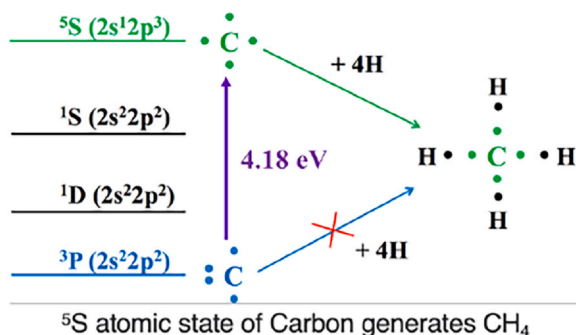


Fig. 1 The sp^3 hybridization of the ground state of the Carbon atom to form CH_4 .

triatomic units, and so on. For instance, in the CH_n series ($n = 1-4$), the following correlations between the ground and the first few excited states of the molecules with the atomic states can be made: $CH(X^2\Pi)$ correlates with $C(^3P) + H(^2S)$, $CH(^4\Sigma^-)$ correlates with $C(^5S) + H(^2S)$, and $CH(^2\Delta)$ correlates with $C(^2D) + H(^2S)$. Therefore the 1-body term for the above three cases is zero, $E[X(^5S)] - E[X(^3P)]$, and $E[X(^2D)] - E[X(^3P)]$, respectively. The same holds for the ground and the excited states of XH_2 , viz. $CH_2(X^3B_1)$ correlates with $C(^5S) + H(^2S)$, $CH_2(a^1A_1)$ correlates with $C(^3P) + H(^2S)$, and so on for CH_3 and CH_4 as explicitly described in Ref.⁶⁷ The fact that the polyatomic ground states correlate with excited states of the constituent atoms has been also reported previously for the $Fe^{2+}(H_2O)_6$ and $Fe^{3+}(H_2O)_6$ clusters⁷⁹ and the $[Fe(SCH_3)_4]^q$ molecules, where $q = -2, -1, +2, +3$.⁸⁰

4. Covalently bonded molecules

The previously described MBE scheme, that incorporates the concept of the in situ electronic state of an atom in a molecule, was used to compute atomization energies ($\Delta E_{atomiz.}$) for the XH_n series ($X = C, Si, Ge, Sn$; $n = 1-4$) at the RCCSD(T)/aug-cc-pVQZ level of theory.⁶⁷ This MBE approach enables the breakdown of the atomization energy into contributions from atoms, dimers, trimers, and higher-order fragments. In this implementation, which defines subsystems based on the breaking of covalent bonds, the 1-B term differs both qualitatively and quantitatively from the commonly used 1-B term in MBE studies of aqueous ionic systems.

As noted earlier, in hydrogen-bonded systems, the 1-B term typically represents the geometrical distortion of molecular fragments from their gas phase structures due to interactions with surrounding molecules or ions. This contribution is relatively small, ranging from a few tenths to a few kcal/mol⁷⁷ and can be indirectly accounted for using infrared (IR) spectroscopy, which detects the red shifts in the vibrational band positions caused by changes in the internal fragment geometry, which can, in turn, be related to the energy penalty of the distorted geometry from the equilibrium one. In contrast, for systems where covalent bonds are broken to define subsystems (“bodies”), the 1-B term reflects the electronic excitation energy required to promote an atom to its in situ electronic state within the molecule. This energy is significantly larger, on the order of a few electron volts (eV) – roughly two orders of magnitude greater than in the hydrogen-bonded case – and is accessible through ultraviolet-visible (UV-Vis) spectroscopy.

The many-body decomposition of the $\Delta E_{\text{atomiz.}}$ for the 3B_1 and 1A_1 states of the XH_2 molecules, where $X = C, Si, Ge, Sn$ is depicted in Figs. 2 and 3. In the case of the 3B_1 states, the in situ X atom is in the 5S state, while in the case of the 1A_1 state the X atom is in its atomic ground state, 3P . The ground state of the CH_2 molecule is X^3B_1 , whereas for the remaining XH_2 , $X = Si-Sn$, molecules their ground state is X^1A_1 . Similar $\Delta E_{\text{atomiz.}}$, 1-B, 2-B, and 3-B terms are observed for the SiH_2 and GeH_2 molecules, while the SnH_2 presents the smallest terms. On the other hand, the CH_2 molecule presents the largest absolute values of energetics. This occurs because the C-H bond is the strongest one comparing to the remaining X-H bonds.⁶⁷ Due to the breaking of covalent bonds, the basis set superposition error (BSSE) is expected to be quite small. Indeed, the BSSE was found to be negligible across all systems in this series, see Fig. 3. It is interesting that in the case of the 1A_1 states, for all XH_2 molecules, the 3-B term was found to further stabilize the molecules.

The many-body decomposition of the $\Delta E_{\text{atomiz.}}$ for the $XH_3(X^2A_1)$ and $XH_4(X^1A_1)$ molecules is shown in Fig. 4. Our application of this MBE framework to the XH_n series reveals an alternating (oscillatory) pattern of positive and negative many-body terms, with eventual convergence as the order of expansion increases. Among these, the two-body (2-B) X-H interaction is consistently the most significant contributor to the binding energy. The strength of this 2-B term correlates well with the X-H bond length, which varies across the series due to geometric differences between the systems. Thus, the CH_n molecules present the largest 2-B terms and the

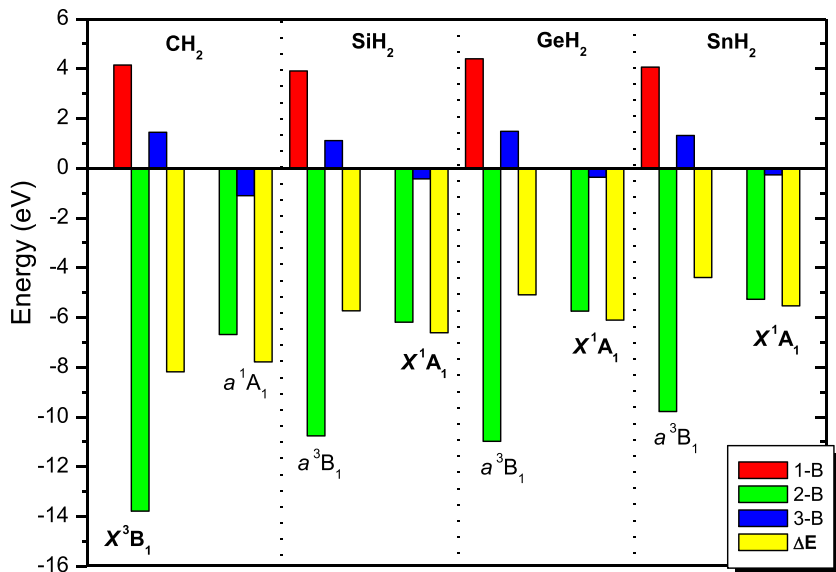


Fig. 2 Many-body decomposition of the ΔE_{atomiz} for the X^3B_1 and a^1A_1 states of the XH_2 , where $X = C, Si, Ge, Sn$ at the RCCSD(T)/aug-cc-pVQZ(-PP)_{Sn} level of theory.

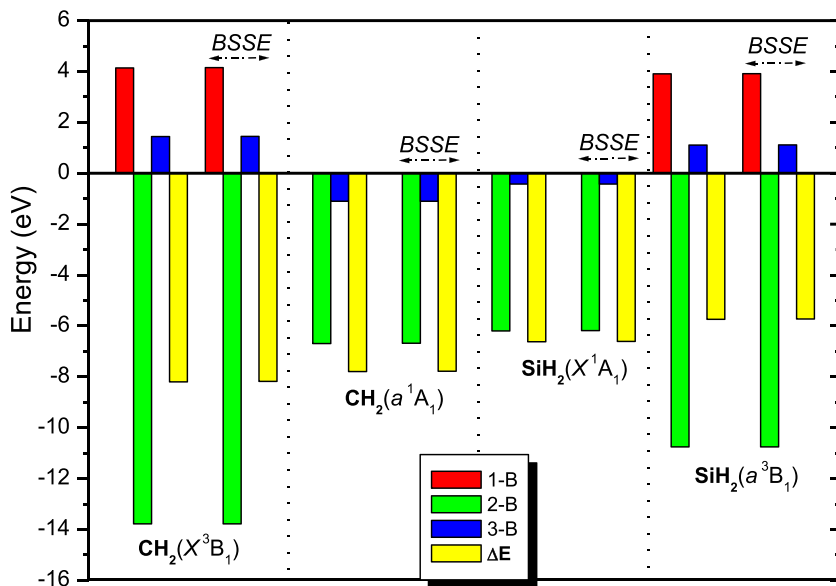


Fig. 3 Many-body decomposition of the ΔE_{atomiz} for the X^3B_1 and a^1A_1 states of the XH_2 , where $X = C$ and Si at the RCCSD(T)/aug-cc-pVQZ(-PP)_{Sn} level of theory with and without BSSE correction.

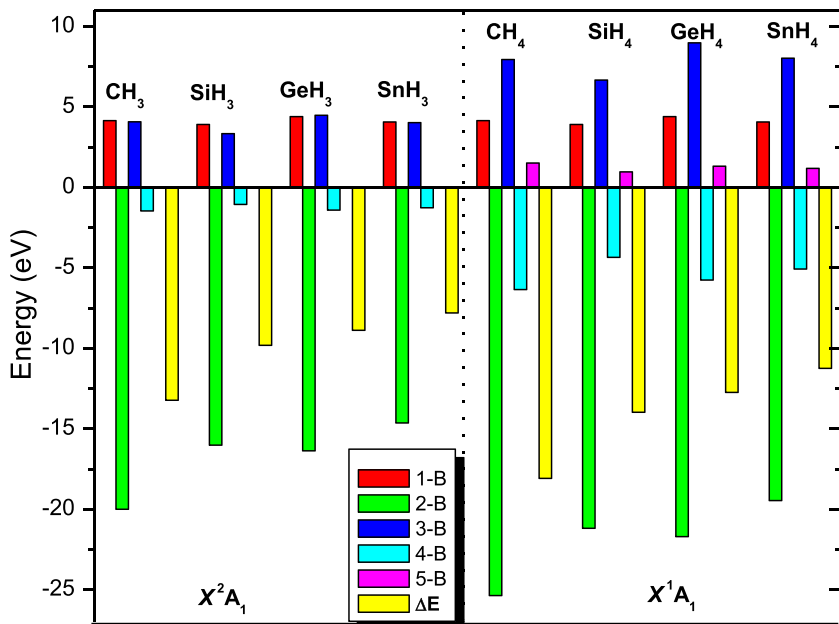


Fig. 4 Many-body decomposition of the $\Delta E_{\text{atomiz.}}$ of the XH_3 (X^2A_1) and XH_4 (X^1A_1) molecules, where $X = \text{C}, \text{Si}, \text{Ge},$ and Sn at the RCCSD(T)/aug-cc-pVQZ-(PP)_{Sn} level of theory.

SnH_n the smallest one, see Fig. 4. Regarding the 3-B terms, which are positive for all XH_3 and XH_4 molecules, Ge is associated with the most positive, i.e., the most destabilizing 3-B terms, since its 2-B terms are similar to the corresponding values of Si, but the $\Delta E_{\text{atomiz.}}$ of Ge molecules are smaller than those of the Si corresponding molecules.

Overall, the MBE analysis for these systems offers an alternative perspective on the so-called “first-row anomaly” in the incremental $\text{H}_{n-1}\text{X}-\text{H}$ bond energies,⁸¹ for which the CH_n compounds ($n = 1-4$) exhibit a different trend compared to their heavier counterparts ($\text{SiH}_n, \text{GeH}_n, \text{SnH}_n$) when these bond energies are evaluated with respect to the respective ground states of each molecule. This apparent “anomaly” arises from a reversal in the ordering of the ground and first excited electronic states between CH_2 (3B_1 ground state, 1A_1 excited state) and XH_2 ($X = \text{Si}, \text{Ge}, \text{Sn}$), which exhibit the opposite ordering (1A_1 ground state, 3B_1 excited state), see Fig. 2. Note that in the XH_2 molecule, the X atom is in an excited 4S atomic state within the triplet 3B_1 electronic state, whereas in the singlet 1A_1 state, the X atom remains in its ground 3P atomic state.

However, when the incremental bond energies are instead evaluated relative to molecular states with consistent in situ atomic configurations, the trends become uniform across all elements in the series, eliminating the basis for a “first-row anomaly”, see Fig. 4.

In addition, the MBE analysis for the H_2O , NH_3 molecules and the H_3O^+ , NH_4^+ cations is shown in Fig. 5. The atoms in all four species are in their atomic ground states, therefore for all 4 species the 1-B term is zero. The MBE decomposition of the atomization energy of the H_2O follows the general trend previously observed for the XH_2 ($^1\text{A}_1$) molecule. Both H_3O^+ and NH_3 follow the same MBE decomposition trend, i.e., both the 2-B and 3-B terms stabilize the species, while the 4-B term destabilizes them slightly. Finally, the MBE pattern for the decomposition of the $\Delta E_{\text{atomiz.}}$ of the NH_4^+ cation follows the general shape of the XH_4 ($^1\text{A}_1$) molecules, except from the fact that the 1-B term is zero, since all atoms are in their ground states. Furthermore, the 2-B is by far the largest term in the MBE with the higher order terms oscillating between positive and negative values and decreasing dramatically in size with increasing rank of the expansion, see Fig. 5.

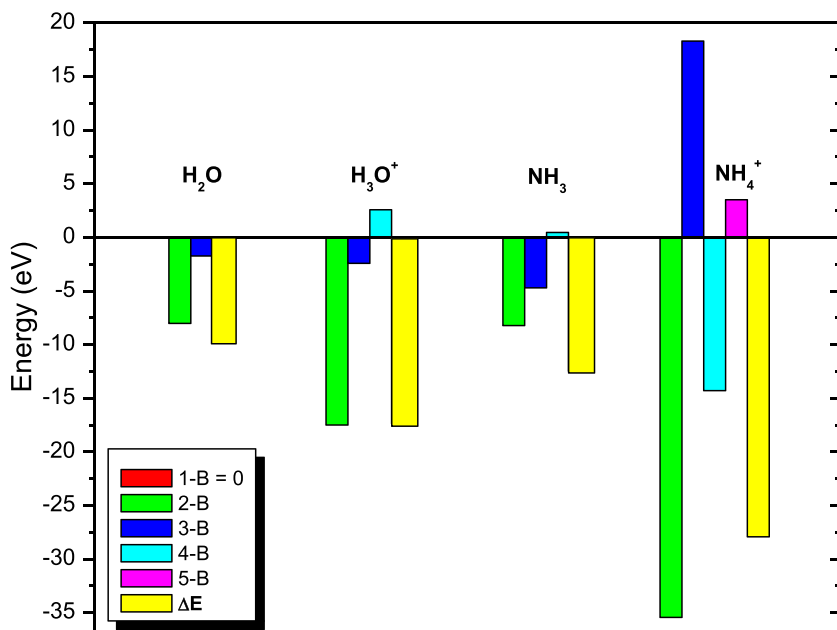


Fig. 5 Many-body decomposition of the $\Delta E_{\text{atomiz.}}$ of the H_2O , H_3O^+ , NH_3 , and NH_4^+ species at the RCCSD/aug-cc-pVTZ level of theory.

Finally, it should be noted that while the present analysis of the MBE of the atomization energy is simplified by the presence of only one heavy atom (N, O, C, Si, Ge, or Sn) per system, it lays the groundwork for extending MBE methodologies beyond hydrogen-bonded networks to include covalent bond dissociation. This expanded framework offers valuable insights into the nature of chemical bonding and can serve as a foundation for more complex systems involving multiple heavy atoms.



5. Metallic clusters

Small metal clusters attract significant attention in physical sciences because of their distinct electronic structures and promising applications in catalysis and other industrial fields. Their binding energies can vary markedly depending on size and geometry, highlighting the influence of non-additive interaction effects. Additionally, cluster size can impact properties such as the emergence of metallic behavior and catalytic activity, as these are closely linked to changes in the energetics of adsorbate interactions. To gain insight into the interatomic forces, electronic structure, and the (non)additive nature of these interactions, it is often useful to express the system's total energy through a many-body decomposition.^{68–70}

Recently, the MBE analysis was applied to clusters of homometallic and heterometallic alkali metals (Li, Na and K), and alkaline earth metals (Be, Mg and Ca).^{69,70} Additionally, alkali metal borides (Li_2B and LiB_2) were also investigated.⁷⁰ Specifically, we have analyzed the non-additive MBE contributions in various mixed metal trimer clusters to understand how the electronic structures of constituent metals influence both the sign (stabilizing or destabilizing) and the magnitude of the two- and three-body (2-B and 3-B) interaction terms. Our focus was on clusters composed of metals with valence electron configurations of ns^1 , ns^2 , and ns^2p^1 , both in homometallic and heterometallic clusters. The calculations were carried out using a variety of theoretical methods, including second order perturbation (MP2), Coupled Cluster (CCSD, CCSD(T)), Complete Active Space Self-Consistent Field (CASSCF), and internally contracted Multi-Reference Configuration Interaction with Single and Double excitations (icMRCISD). Similarly to the previous cases, the BSSE was found to be negligible across all systems studied. Our results suggest that the MBE is highly system-specific, lacking clear trends across different cluster series or

even among different electronic states of the same cluster. To interpret these patterns, we attempted to group the findings based on metal identity, cluster size, and electronic state. Key observations include:

Homonuclear Alkali Metal Clusters (ns^1 configuration; Li_n , Na_n , K_n , $n = 2-5$): as the principal quantum number increases from 2 to 4 (i.e. [He] $2s^1 \rightarrow$ [Ne] $3s^1 \rightarrow$ [Ar] $4s^1$), the MBE displays an oscillating trend: the 2-B and 4-B terms are stabilizing (negative), while the 3-B term is destabilizing (positive), with the magnitude of all terms decreasing along the series.⁷⁰ A strong correlation between higher-order terms (3-B and 4-B) and the pairwise 2-B term at the energy minima suggests the potential for efficient ab initio-based Monte Carlo simulations based on this finding, provided this relationship persists away from equilibrium geometries.⁷⁰

As an example, the many-body decomposition of the $\Delta E_{\text{atomiz.}}$ of the ground states of the Na_3 (doublet), Na_4 (singlet), and Na_5 (doublet) are plotted in Fig. 6(i), where it is shown that the metallic clusters are stabilized by 2-B interactions and destabilized by 3-B contributions. Note that CCSD and CCSD(T) present similar results for $\Delta E_{\text{atomiz.}}$, specifically that about 96 % of the CCSD(T) correlation energy is obtained at the CCSD level. Furthermore, the BSSE corrections are negligible, amounting to <0.3 % of the total binding and therefore they can be neglected.

The many body decomposition for the high spin states of Na_3 (quartet), Na_4 (quintet), and Na_5 (sextet) is shown in Fig. 6(ii). It is very interesting that the high spin structures are stabilized mainly due to the 3-B interaction. Furthermore, the 3-B term for both Na_4 and Na_5 is larger than the $\Delta E_{\text{atomiz.}}$ value. Finally, for the Na_3 the 2-B term slightly stabilizes the cluster, while in the case of the Na_5 the 5-B slightly stabilizes the cluster, see Fig. 6.

The molecular structures of the lowest in energy low and high spin states Na_n , $n = 3-5$, are also depicted in Fig. 6, and it is shown that both Na_4 and Na_5 clusters consist of triangular subunits. In the cases of the high spin is attributed to the negative value of the 3-B term, i.e., it stabilized the cluster. In the case of the low spin states, the 2-B term and 3-B terms show the opposite trend—stabilization via 2-B and 4-B and destabilization via 3-B terms.⁷⁰ however the triangular subunits are preferred.

Heteronuclear Alkali Metal Clusters (ns^1 configuration; Li_3 , Li_2Na , $LiNa_2$, Na_3): in clusters combining metals of similar valence structure but differing in atomic size ($n = 2-3$), the quartet states are predominantly stabilized by the 3-B term, which contributes 131 %, 130 %, 117 %, and 86 % of the binding energy, respectively, at the CCSD/AVTZ level indicating a

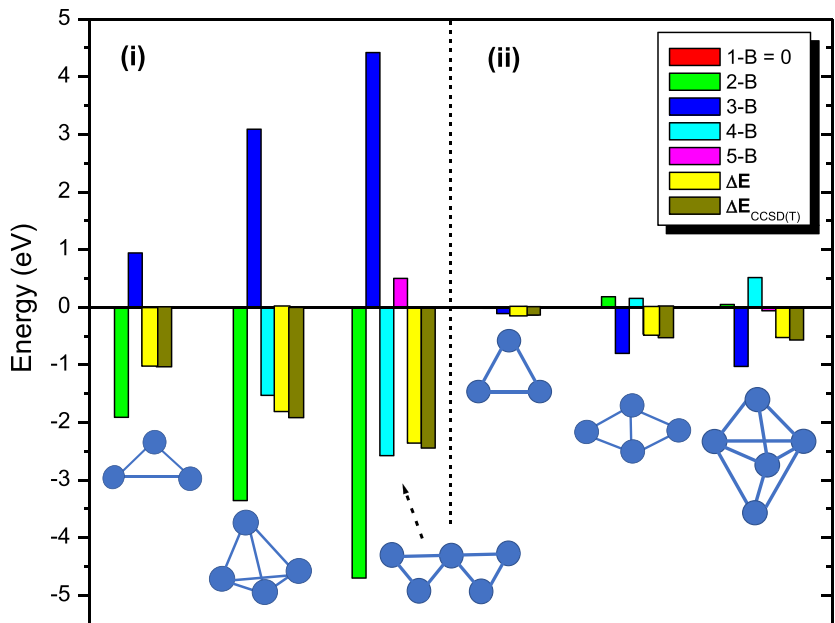


Fig. 6 Many-body decomposition of the ΔE_{atomiz} of the Na_3 , Na_4 , and Na_5 molecules at the CCSD/aug-cc-pVTZ level of theory; (i) ground states of the Na_3 (doublet), Na_4 (singlet), and Na_5 (doublet) and (ii) high spin states of Na_3 (quartet), Na_4 (quintet), and Na_5 (sextet).

destabilizing behavior for the 2-B term, see Fig. 7. The inclusion of higher-order correlation (e.g., CCSD(T)) leads to only minor changes in these contributions.

Heteronuclear Boride Clusters (Li_3 , Li_2B , LiB_2 , B_3): substituting Li (ns^1) with B (ns^2p^1) in the quartet state of Li_3 reduces the 3-B term significantly, contributing 16 % in Li_2B and just 5 % in LiB_2 . In the B_3 cluster, the 3-B term slightly destabilizes the system, amounting to -1 % of the binding energy, see Fig. 7.

Alkaline Earth Metal Clusters (Be_3 , Be_2Mg , BeMg_2 , Mg_3): for these ns^2 configuration clusters, the 3-B term dominates contributing 178 %, 222 %, 253 %, and 132 % of the total ΔE_{atomiz} in their ground states. This indicates that the 2-B term is destabilizing, and the binding is largely due to 3-body interactions, see Fig. 8. The many-body decomposition has been done with respect to the atomic ground states, $\text{Be}(^1\text{S})$, $\text{Mg}(^1\text{S})$ and the diatomic ground states $\text{Be}_2(X^1\Sigma_g^+)$, $\text{Mg}_2(X^1\Sigma_g^+)$, and $\text{BeMg}(X^1\Sigma^+)$. Note that

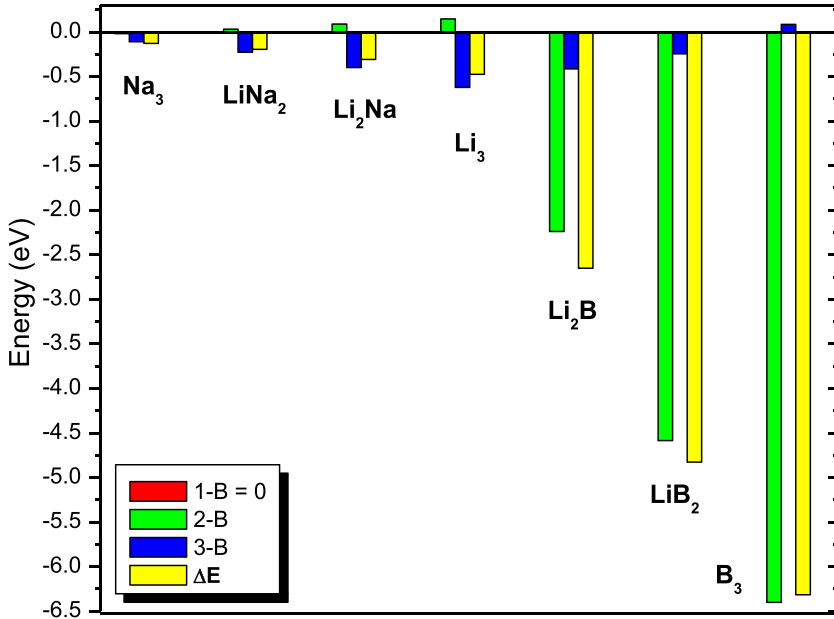
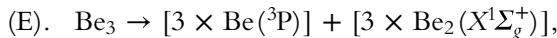
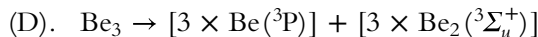
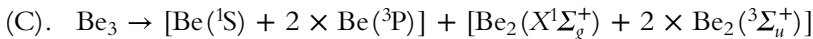
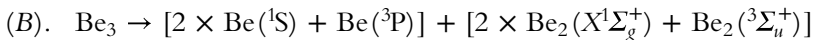
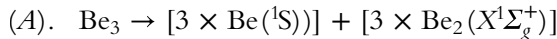


Fig. 7 Many-body decomposition of the $\Delta E_{\text{atomiz.}}$ of the Li_3 , Li_2Na , LiNa_2 , Na_3 , Li_2B , LiB_2 , B_3 molecules at the CCSD/aug-cc-pVTZ level of theory.

these alkaline earth metal clusters present a significant sp hybridization. Therefore, if this hybridization is considered as an atomic excitation the MBE decomposition will change. For instance, in the case of the Be_3 cluster, five decomposition channels (a)-(e) can be considered, viz.



and the corresponding many-body decomposition of the $\Delta E_{\text{atomiz.}}$ is shown in Fig. 9. Thus, when the in situ state of the atom cannot be clearly assigned, the many-body decomposition of the $\Delta E_{\text{atomiz.}}$ may have different interpretations.

Alkaline Earth Metal Clusters (Be_n , Mg_n , Ca_n , $n = 2-6$): several isomers of M_n ($\text{M}=\text{Be}, \text{Mg}, \text{Ca}$) were investigated and it was found that regardless of

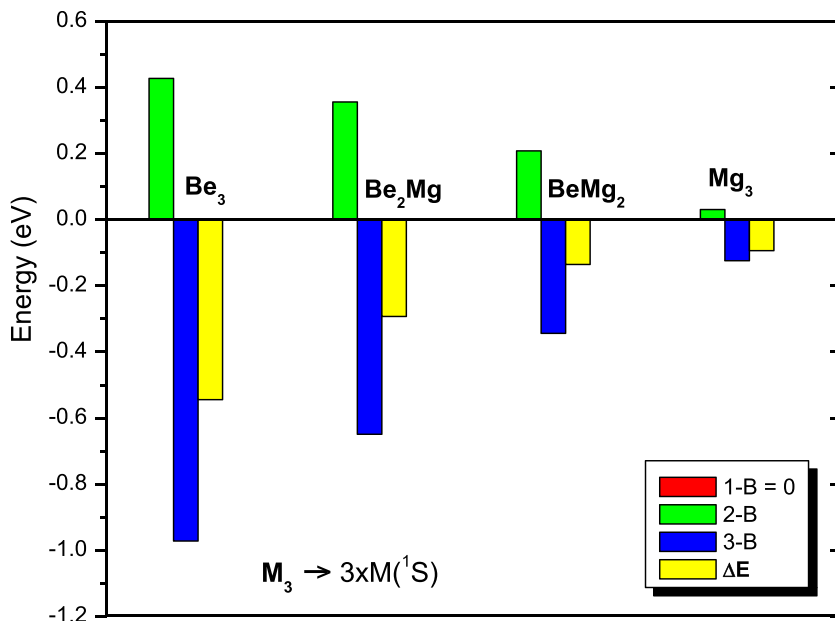


Fig. 8 Many-body decomposition of the $\Delta E_{\text{atomiz.}}$ of the Be_3 , Be_2Mg , BeMg_2 , and Mg_3 molecules with respect to $3 \times \text{M}(^1\text{S})$ at the RCCSD/aug-cc-pVTZ level of theory.

the level of theory considered, the calculations consistently indicated that these alkaline earth metal clusters exhibit negligible 2-B interactions, with binding predominantly arising from 3-B effects. In some cases, higher-order interactions (4-B, 5-B, etc.) also contributed, though their impact diminished gradually and displayed an oscillatory trend beyond the 3-B term. Quasi-atomic orbital analysis revealed how the electronic orbital character evolves from the dimer to the trimer configurations, highlighting the critical role of the third atom in establishing the overall binding energy of the cluster.

Overall, replacing ns^1 with ns^2p^1 metals tends to weaken the 3-B contribution while enhancing stabilization via 2-B interactions. Additionally, increasing atomic size reduces the significance of 3-B terms due to the longer bond lengths. Finally, it should be noted that the MBE analysis of metallic clusters lays the foundation for extending the MBE to coordination chemistry, where such decomposition can offer a deeper physical insight into metal–ligand interactions.

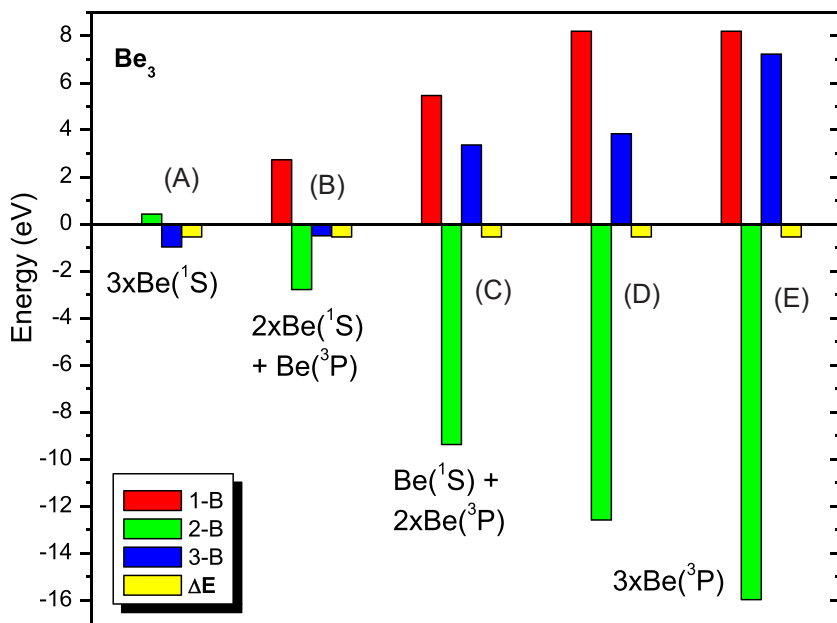


Fig. 9 Many-body decomposition of the $\Delta E_{\text{atomiz.}}$ of the Be_3 with respect to different dissociation channels (A) $\text{Be}_3 \rightarrow [3 \times \text{Be}(^1\text{S})] + [3 \times \text{Be}_2 (^1\Sigma_g^+)]$; (B) $\text{Be}_3 \rightarrow [2 \times \text{Be}(^1\text{S}) + \text{Be}(^3\text{P})] + [2 \times \text{Be}_2 (^1\Sigma_g^+) + \text{Be}_2(^3\Sigma_u^+)]$; (C) $\text{Be}_3 \rightarrow [\text{Be}(^1\text{S}) + 2 \times \text{Be}(^3\text{P})] + [\text{Be}_2 (^1\Sigma_g^+) + 2 \times \text{Be}_2(^3\Sigma_u^+)]$; (D) $\text{Be}_3 \rightarrow [3 \times \text{Be}(^3\text{P})] + [3 \times \text{Be}_2(^3\Sigma_u^+)]$; (E) $\text{Be}_3 \rightarrow [3 \times \text{Be}(^3\text{P})] + [3 \times \text{Be}_2 (^1\Sigma_g^+)]$ at the RCCSD/aug-cc-pVTZ level of theory.

6. Light nuclei

Similarly, in nuclear physics, the MBE plays a crucial role in understanding and calculating the properties of atomic nuclei, which are systems made up of many strongly interacting nucleons, i.e., protons and neutrons.⁷¹ Nuclei are many-body quantum systems held by the strong nuclear force, which is short-range, complex, non-linear and it involves multi-body (i.e. not just pairwise additive) correlations. Thus, the exact quantum mechanical solution of the energy problem is challenging for nuclei beyond the lightest ones. The MBE allows for the decomposition of the total energy of a nucleus into the individual 1-B terms (individual nucleons), 2-B interactions (nucleon pairs), 3-B interactions (nucleon triples), and so on. The truncation of the series at a manageable order (e.g., 2-B or 3-B) is very common, by assuming that the higher-order terms are less significant. As a result, the calculation of the full system is evitable. The

commonly used methods are *ab-initio* coupled-cluster theory, configuration interaction methods, quantum Monte Carlo as well as empirical and semi-empirical simulations.^{71,73}

Note that the nuclear many-body problem is one of the first many particle systems where quantum statistics has been applied almost a century ago.⁷³ Since degeneracy and strong interaction represent challenges, new concepts such as quasi-particles and bound state formation have been introduced and investigated via new methodologies, i.e., Green's functions, Feynman diagram techniques, etc. Other many-body systems, such as solid-state physics, strongly coupled Coulomb plasmas and warm dense matter, adapted these methods and further developed them.^{71-73,82,83}

Recently, the MBE concept previously applied to hydrogen bonded, van der Waals bonded systems or molecular systems was also applied to light nuclear systems, i.e., ^2H , ^3H and ^3He by considering the nucleonic degrees of freedom as fundamental in the expansion.⁷² The MBE analysis was based on the Pauli Nucleonic Dynamics (PND) model,⁷² which is a simple anti-symmetrized dynamical formulation driven by the Constrained Molecular Dynamics (CoMD) model.⁸⁴ Specifically, the Anti-symmetrized Molecular Dynamics (AMD)⁸⁵ approach was used to calculate the total three-body contribution to the interaction energy of ^3H and ^3He . In the MBE extension to light nuclear systems, the 1-B terms correspond to the monomer energies, which are the kinetic energies (T_n or T_p , where n denotes the neutrons and p the protons) of the nucleons, the 2-B terms are the two body potential energy interactions (V_{pn} or V_{pp} or V_{nn}), while the 3-B term is the difference between total energy (E_{tot}) and the sum of 1-B and 2-B terms. Assuming that the total energy for the trimers is the experimentally measured energy of the corresponding nuclear system (E_{exp}), while the sum of the 1-B and 2-B terms are calculated by the PND model, the 3-B term is obtained via Eq. (6). To accurately simulate the interactions within the two- and three-nucleon systems, we introduced a new potential term incorporating spin-isospin dependence.⁷² The limited set of free parameters was calibrated using properties of the deuteron. Further details regarding the PND model are given in ref.⁷²

The MBE of the binding energy for the light nuclei $^2\text{H}(p\uparrow n\uparrow)$ is $E = T_p + T_n + V_{pn}$, for the $^3\text{H}(p\uparrow n\uparrow n\downarrow)$ is $E = T_p + T_n + T'_n + V_{pn} + V'_{pn} + V_{nn} + E_{pnn}^3$ and for $^3\text{He}(p\uparrow p\downarrow n\uparrow)$ is $E = T_p + T'_p + T_n + V_{pn} + V'_{pn} + V_{pp} + E_{ppn}^3$. The sum of 1-B terms, i.e., the kinetic energies of the involved p and n species, is positive. The sum of 2-B terms, i.e., the potential energy, is negative, while their sum is also negative showing that the calculated

nuclear systems are bound, see Fig. 10. For ${}^2\text{H}$ the PND total energy is calculated at -2.31 MeV, in very good agreement with the experimental value of -2.225 MeV.⁸⁶ For ${}^3\text{H}$ and ${}^3\text{He}$, the PND model predicts that the $\Sigma[E(1\text{-B})+E(2\text{-B})]$ terms is -6.97 ± 0.21 MeV and -6.19 ± 0.21 MeV respectively, while the 3-body term is 1.51 ± 0.21 MeV and 1.53 ± 0.21 MeV, respectively. This suggests that the 3-B terms are between 16–23 % of the total energy, i.e., they to contribute significantly in the total energy of the species.⁷² Overall, the MBE for light nuclei resembles the MBE for water clusters, except for the significantly larger 1-B term for the light nuclei, however, the 2-B terms are negative and larger than the 1-B terms. It is worth mentioning that in the water trimer,⁴ the 3-B term amounts to $\sim 18\%$ of its total binding energy, i.e., it is similar to the % contribution of the 3-B term in the ${}^3\text{H}$ and ${}^3\text{He}$ nuclei.⁷²

Finally, it should be noted that in the PND model the full spin dependence of the interaction has not yet been addressed. Future work will focus on enhancing the PND model by incorporating a spin-orbit interaction to achieve a more precise description of nuclear systems, as well as enabling the extraction of additional ground state properties, such as neutron skins and radii, that are relevant to nuclear structure studies. Additionally, it would be valuable to apply the MBE approach to heavier

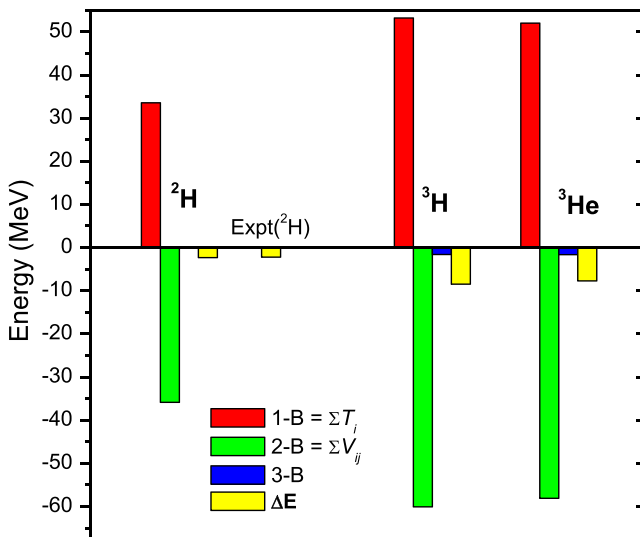


Fig. 10 Many-body decomposition of the energy for the light nuclei ${}^2\text{H}(\text{p}\uparrow\text{n}\uparrow)$, ${}^3\text{H}(\text{p}\uparrow\text{n}\uparrow\text{n}\downarrow)$ and ${}^3\text{He}(\text{p}\uparrow\text{p}\downarrow\text{n}\uparrow)$.

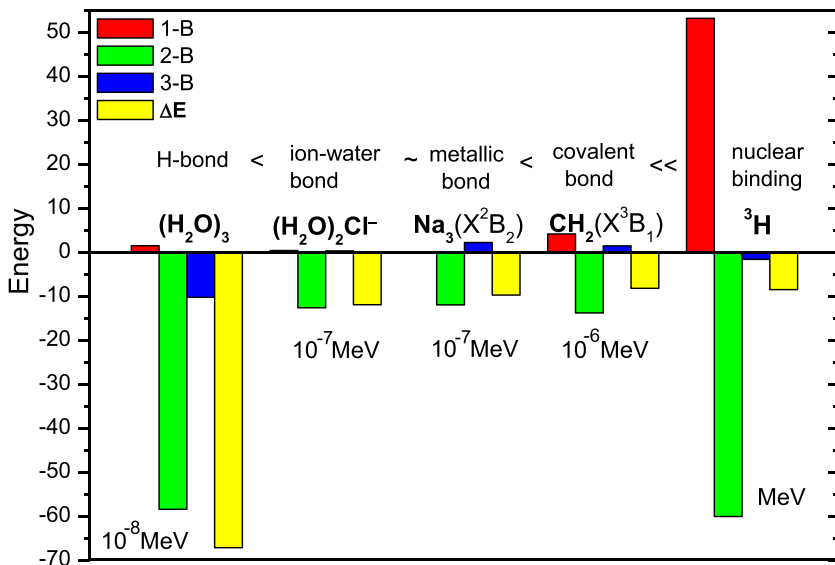


Fig. 11 MBE of the binding energy of five different bonded trimers having different order of magnitude interaction energies in eV.

nuclei, where a larger number of protons and neutrons are present, to evaluate the convergence behavior of the MBE and assess the significance of higher-order terms.

7. Conclusions

The MBE concept can be successfully used to analyze and understand the composition of interatomic and intermolecular interactions. In this chapter, the application of MBE is extended into (a) systems that are formed via covalent bonds, (b) metal clusters and (c) light nuclei. These three types of systems present significant challenges compared to the hydrogen bonded or van der Waals bonded systems. Below we analyze the prerequisites for a meaningful application of the MBE to various systems exhibiting different bonding characteristics.

- i. **Hydrogen bonded or van der Waals bonded systems:** usually, a single reference method is adequate, while the use of an augmented basis set with diffusion functions and the consideration of BSSE correction are necessary.

- ii. **Covalently bonded systems:** it is crucial to define the in situ atomic states of the individual atoms, while depending on the type of the studied systems either single reference or multireference methods are needed. The inclusion of the BSSE correction is not necessary.
- iii. **Metallic systems:** they pose additional challenges due to their complex electronic structure and strong short-range interactions. Accurately capturing the multi-coordinated bonding typical of metals often requires the consideration of both static and dynamic electron correlation effects, as well as the careful handling of spin multiplicities in intermediate structures involving open-shell metal species. The inclusion of the BSSE correction is not necessary.
- iv. **Light nuclei:** An MBE analysis based on the Pauli Nucleonic Dynamics (PND) model, which is a simple anti-symmetrized dynamical formulation driven by the Constrained Molecular Dynamics (CoMD) model was adequate for the light nuclei. However, the full spin dependence of the interaction should also be included to achieve a more precise description of nuclear systems, as well as enabling the extraction of additional ground state properties, such as neutron skins and radii, that are relevant to nuclear structure studies.

The concept of the MBE implementation for the cases of covalent bonded systems or the metallic ones is that the in situ atomic electronic state of an atom in a molecule determines the one-body term. Specifically, the 1-B term corresponds to the required energy for the promotion of the atom from the ground to its in situ state. For the cases of light nuclear systems, the kinetic energy of each nucleon corresponds to the 1-B term. Note that in the hydrogen bonded or van der Waals bonded systems, the 1-B term corresponds to the deformation energy of each species.

Fig. 11 shows the MBE of the binding energy of five different bonded trimers that exhibit values ranging over 8 orders of magnitude in MeV. These are the hydrogen-bonded $(\text{H}_2\text{O})_3$ cluster,⁴ the ion-water hydrogen bonded $\text{Cl}^-(\text{H}_2\text{O})_2$ cluster,⁹ the metallic Na_3 cluster,⁷⁰ the covalently bonded CH_2 molecule,⁶⁷ and the light ^3H nucleus.⁷² These trimer species are bound together with interaction energies spanning 8 orders of magnitude, ranging from 7×10^{-7} to 8 MeV. In all cases, it is found that the 1-B terms are positive destabilizing the system, while the 2-B terms stabilize the trimer species. As regards the 3-B term, it is either stabilizing (negative) or destabilizing (positive) depending on the system. In most cases, the stabilization due to the 3-B term is small; however, in metallic clusters, the

3-B terms significantly stabilize the high spin multiplicity states of a cluster formed by the ns^1 metal atoms and the low spin states of a cluster formed by the ns^2 metal atoms.

We envision that the concept of the MBE can be extended into more complicated systems, such as coordination complexes and biomolecules. Up to now, fragmentation methodologies for breaking covalent bond for large systems have been already proposed, and the fragments are groups of atoms, or molecular systems contrary to our study where the “body” is an atom or nucleons. Specifically, for largest organic molecules, a scheme for molecular fragmentation has been proposed by generating a hierarchy of molecular fragmentations, such as $-CH_2-$ in the case of an alkane.⁸⁷ For macromolecules like proteins, a scheme has been reported to compute the interaction energy,⁸⁸ where the protein is decomposed into individual amino acid-based fragments. Furthermore, there are other fragmentation methods^{89,90} that they are based on a non-overlapping MBE protocol and have been applied to biomolecular systems such as G protein-coupled receptors (GPCR)–ligand crystal structures, representing different branches of the GPCR genome⁸⁹ or enzyme–substrate.⁹⁰ In the present MBE scheme, the “body” consists of the atoms involved in the molecular systems. This scheme can provide a more detailed analysis at the atomic level and can be even applied or integrated with machine learning techniques to provide a forward-looking edge in the analysis of the chemical bonding in a wide variety of chemical environments.

Acknowledgments

DT acknowledge computational time granted from the Greek Research & Technology Network (GRNET) in the National HPC facility ARIS under project ID pr015035-TrMeCo. SSX was supported by the Center for Scalable Predictive Methods for Excitations and Correlated Phenomena (SPEC), which is funded by the U.S. Department of Energy (DOE), Office of Science, Basic Energy Sciences (BES), Chemical Sciences, Geosciences, and Biosciences Division (CSGB), as part of the Computational Chemical Sciences (CCS) program under FWP 70942 at Pacific Northwest National Laboratory (PNNL), a multi-program national laboratory operated for DOE by Battelle. This research also used resources of the National Energy Research Scientific Computing Center, which is supported by the Office of Science of the U.S. Department of Energy under Contract No. DE-AC02-05CH11231.

References

1. Roberts, F.; Tesman, B. *Applied Combinatorics*; 2nd ed.; CRC Press, 2009, .
2. Hankins, D.; Moskowitz, J. W.; Stillinger, F. H., Jr. *J. Chem. Phys.* **1970**, *53*, 4544–4554.

- Xantheas, S. S.; Dunning, T. H. The Structure of the Water Trimer from Ab Initio Calculations. *J. Chem. Phys.* **1993**, *98*, 8037–8040.
- Xantheas, S. S. Ab-Initio Studies of Cyclic Water Clusters $(\text{H}_2\text{O})_n$, $n=1-6$. 2. Analysis of Many-Body Interactions. *J. Chem. Phys.* **1994**, *100*, 7523–7534.
- Gordon, M. S.; Fedorov, D. G.; Pruitt, S. R.; Slipchenko, L. V. Fragmentation Methods: A Route to Accurate Calculations on Large Systems. *Chem. Rev.* **2012**, *112*, 632–672.
- Richard, R. M.; Lao, K. U.; Herbert, J. M. Understanding the Many-Body Expansion for Large Systems. I. Precision Considerations. *J. Chem. Phys.* **2014**, *141*, 014108141.
- Liu, J. F.; He, X. Fragment-Based Quantum Mechanical Approach to Biomolecules, Molecular Clusters, Molecular Crystals and Liquids. *Phys. Chem. Chem. Phys.* **2020**, *22*, 12341–12367.
- Xantheas, S. S.; Dunning, T. H. structures and Energetics of $\text{F}-(\text{H}_2\text{O})_n$, $n=1-3$, Clusters from Ab-Initio Calculations. *J. Chem. Phys.* **1994**, *98*, 13489–13497.
- Xantheas, S. S. Quantitative Description of Hydrogen Bonding in Chloride-Water Clusters. *J. Phys. Chem.* **1996**, *100*, 9703–9713.
- Hodges, M. P.; Stone, A. J.; Xantheas, S. S. Contribution of Many-Body Terms to the Energy for Small Water Clusters: A Comparison of Ab Initio Calculations and Accurate Model Potentials. *J. Phys. Chem. A* **1997**, *101*, 9163–9168.
- Xantheas, S. S. Cooperativity and Hydrogen Bonding Network in Water Clusters. *Chem. Phys.* **2000**, *258*, 225–231.
- Tzeli, D.; Mavridis, A.; Xantheas, S. S. A First Principles Study of the Acetylene–Water Interaction. *J. Chem. Phys.* **2000**, *112*, 6178–6189.
- Tzeli, D.; Mavridis, A.; Xantheas, S. S. First Principles Examination of the Acetylene–Water Clusters, $\text{HCCH}-(\text{H}_2\text{O})_x$, $x = 2, 3$, and 4. *J. Phys. Chem. A* **2002**, *106*, 11327–11337.
- Richard, R. M.; Herbert, J. M. Many-Body Expansion with Overlapping Fragments: Analysis of Two Approaches. *J. Chem. Theory Comput.* **2013**, *9*, 1408–1416.
- Lao, K. U.; Liu, K. Y.; Richard, R. M.; Herbert, J. M. Understanding the Many-Body Expansion for Large Systems. II. Accuracy Considerations. *J. Chem. Phys.* **2016**, *144*, 164105.
- Liu, J.; Herbert, J. M. Pair-Pair Approximation to the Generalized Many-Body Expansion: An Alternative to the Four-Body Expansion for Ab Initio Prediction of Protein Energetics via Molecular Fragmentation. *J. Chem. Theory Comput.* **2016**, *12*, 572–584.
- Liu, J.; Herbert, J. M. Energy-Screened Many-Body Expansion: A Practical Yet Accurate Fragmentation Method for Quantum Chemistry. *J. Chem. Theory Comput.* **2020**, *16*, 475–487.
- Christie, R. A.; Jordan, K. D. Intermolecular Forces and Clusters II. In *Structure and Bonding*; Wales, D. J., Ed.; **2005**; pp. , 27–41.
- Dahlke, E. E.; Truhlar, D. G. Electrostatically Embedded Many-Body Expansion for Simulations. *J. Chem. Theory Comput.* **2008**, *4*, 1–6.
- Ouyang, J. F.; Cvitkovic, M. W.; Bettens, R. P. A. Trouble with the Many-Body Expansion. *J. Chem. Theory Comput.* **2014**, *10*, 3699–3707.
- Prasad, S.; Lee, J.; Head-Gordon, M. Polarized Many-Body Expansion: A Perfect Marriage Between Embedded Mean-Field Theory and Variational Many-Body Expansion. *Abstracts of Papers of the American Chemical Society* **2019**, 257.
- Collins, M. A.; Cvitkovic, M. W.; Bettens, R. P. A. The Combined Fragmentation and Systematic Molecular Fragmentation Methods. *Acc. Chem. Res.* **2014**, *47*, 2776–2785.
- Collins, M. A.; Bettens, R. P. A. Energy-Based Molecular Fragmentation Methods. *Chem. Rev.* **2015**, *115*, 5607–5642.

24. Chen, W.; Gordon, M. S. Energy Decomposition Analyses for Many-Body Interaction and Applications to Water Complexes. *J. Phys. Chem.* **1996**, *100*, 14316–14328.
25. Heindel, J. P.; Yu, Q.; Bowman, J. M.; Xantheas, S. S. Benchmark Electronic Structure Calculations for $\text{H}_3\text{O}^+(\text{H}_2\text{O})_n$, $n = 0-5$, Clusters and Tests of an Existing 1,2,3-Body Potential Energy Surface with a New 4-Body Correction. *J. Chem. Theory Comput.* **2018**, *14*, 4553–4566.
26. Heindel, J. P.; Herman, K. M.; Xantheas, S. S. Many-Body Effects in Aqueous Systems: Synergies Between Interaction Analysis Techniques and Force Field Development. *Ann. Rev. Phys. Chem.* **2023**, *74*, 337–360.
27. Herman, K. M.; Xantheas, S. S. An Extensive Assessment of the Performance of Pairwise and Many-Body Interaction Potentials in Reproducing Ab Initio Benchmark Binding Energies for Water Clusters $n = 2-25$. *Phys. Chem. Chem. Phys.* **2023**, *25*, 7120–7143.
28. Heindel, J. P.; Xantheas, S. S. The Many-Body Expansion for Aqueous Systems Revisited: I. Water-Water Interactions. *J. Chem. Theory Comput.* **2020**, *16*, 6843–6855.
29. Heindel, J. P.; Xantheas, S. S. The Many-Body Expansion for Aqueous Systems Revisited: II. Alkali Metal and Halide Ion-Water Interactions. *J. Chem. Theory Comput.* **2021**, *17*, 2200–2216.
30. Herman, K. M.; Heindel, J. P.; Xantheas, S. S. The Many-Body Expansion for Aqueous Systems Revisited: III. Hofmeister Ion-Water Interactions. *J. Chem. Theory Comput.* **2021**, *23*, 11196–11210.
31. Heindel, J. P.; Xantheas, S. S. Molecular Dynamics Driven by the Many-Body Expansion (MBE-MD). *J. Chem. Theory Comput.* **2021**, *17*, 7341–7352.
32. Herman, K. M.; Xantheas, S. S. A Formulation of the Many-Body Expansion (MBE) for Periodic Systems: Application to Several Ice Phases. *J. Phys. Chem. Lett.* **2023**, *14*, 989–999.
33. Xantheas, S. S.; Burnham, C. J.; Harrison, R. J. Development of Transferable Interaction Models for Water. II. Accurate Energetics of the First Few Water Clusters from First Principles. *J. Chem. Phys.* **2002**, *116*, 1493–1499.
34. Burnham, C. J.; Xantheas, S. S. Development of Transferable Interaction Models for Water. IV. A Flexible, All-Atom Polarizable Potential (TTM2-F) Based on Geometry Dependent Charges Derived From An Ab Initio Monomer Dipole Moment Surface. *J. Chem. Phys.* **2002**, *116*, 5115–5124.
35. Fanourgakis, G. S.; Xantheas, S. S. The Flexible, Polarizable, Thole-Type Interaction Potential for Water (TTM2-F) Revisited. *J. Phys. Chem. A* **2006**, *110*, 4100–4106.
36. Fanourgakis, G. S.; Xantheas, S. S. Development of Transferable Interaction Potentials for Water. V. Extension of the Flexible, Polarizable, Thole-Type Model Potential (TTM3-F, v. 3.0) to Describe the Vibrational Spectra of Water Clusters and Liquid Water. *J. Chem. Phys.* **2008**, *128*.
37. Babin, V.; Leforestier, C.; Paesani, F. Development of a "First Principles" Water Potential with Flexible Monomers: Dimer Potential Energy Surface, VRT Spectrum, and Second Virial Coefficient. *J. Chem. Theory Comput.* **2013**, *9*, 5395–5403.
38. Babin, V.; Medders, G. R.; Paesani, F. Development of a "First Principles" Water Potential with Flexible Monomers. II: Trimer Potential Energy Surface, Third Virial Coefficient, and Small Clusters. *J. Chem. Theory Comput.* **2014**, *10*, 1599–1607.
39. Medders, G. R.; Gotz, A. W.; Morales, M. A.; Bajaj, P.; Paesani, F. On the Representation of Many-Body Interactions in Water. *J. Chem. Phys.* **2015**, *143*.
40. Arismendi-Arrieta, D. J.; Riera, M.; Bajaj, P.; Prosimi, R.; Paesani, F. i-TTM Model for Ab Initio-Based Ion-Water Interaction Potentials. 1. Halide-Water Potential Energy Functions. *J. Phys. Chem. B* **2016**, *120*, 1822–1832.

41. Reddy, S. K., et al. On the Accuracy of the MB-pol Many-Body Potential for Water: Interaction Energies, Vibrational Frequencies, and Classical Thermodynamic and Dynamical Properties from Clusters to Liquid Water and Ice. *J. Chem. Phys.* **2016**, *145*.
42. Riera, M.; Gotz, A. W.; Paesani, R. The i-TTM Model for Ab Initio-Based ion-Water Interaction Potentials. II. Alkali Metal Ion-Water Potential Energy Functions. *Phys. Chem. Chem. Phys.* **2016**, *18*, 30334–30343.
43. Wang, Y. M.; Bowman, J. M. Towards an Ab Initio Flexible Potential for Water, and Post-Harmonic Quantum Vibrational Analysis of Water Clusters. *Chem. Phys. Lett.* **2010**, *491*, 1–10.
44. Conte, R.; Qu, C.; Bowman, J. M. Permutationally Invariant Fitting of Many-Body, Non-Covalent Interactions with Application to Three-Body Methane-Water-Water. *J. Chem. Theory Comput.* **2015**, *11*, 1631–1638.
45. Samanta, A. K.; Wang, Y. M.; Mancini, J. S.; Bowman, J. M.; Reisler, H. Energetics and Predissociation Dynamics of Small Water, HCl, and Mixed HCl-Water Clusters. *Chem. Rev.* **2016**, *116*, 4913–4936.
46. Schwan, R., et al. Observation of the Low-Frequency Spectrum of the Water Trimer as a Sensitive Test of the Water-Trimer Potential and the Dipole-Moment Surface. *Angew. Chem. -Inter. Ed.* **2020**, *59*, 11399–11407.
47. Nandi, A., et al. A CCSD(T)-Based 4-Body Potential for Water. *J. Phys. Chem. Lett.* **2021**, *12*, 10318–10324.
48. Herman, K. M.; Stone, A. J.; Xantheas, S. S. A Classical Model for Three-Body Interactions in Aqueous Ionic Systems. *J. Chem. Phys.* **2022**, *157*, 024101.
49. Herman, K. M.; Stone, A. J.; Xantheas, S. S. Accurate Calculation of Many-Body Energies in Water Clusters Using a Classical Geometry-Dependent Induction Model. *J. Chem. Theory Comput.* **2023**, *19*, 6805–6815.
50. Gadre, S. R.; Shirsat, R. N.; Limaye, A. C. Molecular Tailoring Approach for Simulation of Electrostatic Properties. *J. Phys. Chem.* **1994**, *98*, 9165–9169.
51. Yeole, S. D.; Gadre, S. R. Molecular Cluster Building Algorithm: Electrostatic Guidelines and Molecular Tailoring Approach. *J. Chem. Phys.* **2011**, *134*, 084111.
52. Sahu, N.; Gadre, S. R. Molecular Tailoring Approach: A Route for ab Initio Treatment of Large Clusters. *Accounts of Chemical Research* **2014**, *47*, 2739–2747.
53. Deshmukh, M. M.; Gadre, S. R. Molecular Tailoring Approach for the Estimation of Intramolecular Hydrogen Bond Energy. *Molecules* **2021**, *26*, 2928.
54. Sahu, N., et al. Low Energy Isomers of (H₂O)₂₅ from a Hierarchical Method Based on Monte Carlo Temperature Basin Paving and Molecular Tailoring Approaches Benchmarked by MP2 Calculations. *J. Chem. Phys.* **2014**, *141*, 164304.
55. Wang, Z. L.; Han, Y. Q.; Li, J. J.; He, X. Combining the Fragmentation Approach and Neural Network Potential Energy Surfaces of Fragments for Accurate Calculation of Protein Energy. *J. Phys. Chem. B* **2020**, *124*, 3027–3035.
56. Shen, C. F.; Jin, X. S.; Glover, W. J.; He, X. Accurate Prediction of Absorption Spectral Shifts of Proterorhodopsin Using a Fragment-Based Quantum Mechanical Method. *Molecules* **2021**, *26*, 4486.
57. Hirata, S. Fast Electron Correlation Methods for Molecular Clusters in the Ground and Excited States. *Mol. Phys.* **2005**, *103*, 2255–2265.
58. He, X.; Sode, O.; Xantheas, S. S.; Hirata, S. Second-Order Many-Body Perturbation Study of Ice IH. *J. Chem. Phys.* **2012**, *137*.
59. Boschen, J. S.; Theis, D.; Ruedenberg, K.; Windus, T. L. Correlation Energy Extrapolation by Many-Body Expansion. *J. Phys. Chem. A* **2017**, *121*, 836–844.
60. Bytautas, L.; Ruedenberg, K. Correlation Energy Extrapolation by Intrinsic Scaling. III. Compact Wave Functions. *J. Chem. Phys.* **2004**, *121*, 10852–10862.
61. Bytautas, L.; Ruedenberg, K. Correlation Energy Extrapolation by Intrinsic Scaling. I. Method and Application to the Neon Atom. *J. Chem. Phys.* **2004**, *121*, 10905–10918.

62. Bytautas, L.; Ruedenberg, K. Correlation Energy Extrapolation by Intrinsic Scaling. IV. Accurate Binding Energies of the Homonuclear Diatomic Molecules Carbon, Nitrogen, Oxygen and Fluorine. *J. Chem. Phys.* **2005**, *122*, 154110.
63. Bytautas, L.; Ruedenberg, K. Correlation Energy Extrapolation by Intrinsic Scaling. V. Electronic Energy, Atomization Energy, and Enthalpy of Formation of Water. *J. Chem. Phys.* **2006**, *124*, 174304.
64. Bytautas, L.; Ruedenberg, K. Accurate Ab Initio Potential Energy Curve of O-2. I. Nonrelativistic Full Configuration Interaction Valence Correlation by the Correlation Energy Extrapolation by Intrinsic Scaling Method. *J. Chem. Phys.* **2010**, *132*, 074109.
65. Stoll, H.; Paulus, B.; Fulde, P. On the Accuracy of Correlation-Energy Expansions in Terms of Local Increments. *J. Chem. Phys.* **2005**, *123*, 144108.
66. Paulus, B. The Method of Increments - A Wavefunction-Based Ab Initio Correlation Method for Solids. *Phys. Rep.-Rev. Sec. Phys. Lett.* **2006**, *428*, 1-52.
67. Tzeli, D.; Xantheas, S. S. Breaking Covalent Bonds in the Context of the Many-Body Expansion (MBE): I. The Purported "first row anomaly" in XH_n ($X = C, Si, Ge, Sn; n = 1-4$). *J. Chem. Phys.* **2022**, *156*, 244303.
68. Higgins, J.; Hollebeek, T.; Reho, J., et al. Maciej Gutowski, On the Importance of Exchange Effects in Three-Body Interactions: The Lowest Quartet State of Na_3 . *J. Chem. Phys.* **2000**, *112*, 5751-5761.
69. Mato, J.; Tzeli, D.; Xantheas, S. S. The Many-Body Expansion for Metals I: The Alkaline Earth metals Be, Mg, and Ca. *J. Chem. Phys.* **2022**, *157*, 084313.
70. Tzeli, D.; Mato, J.; Xantheas, S. S. The Many-Body Expansion for Metals: II. Non-Additive Terms in Clusters Comprised of Metals with ns^1 , ns^2 and ns^2p^1 Configurations. *J. Phys. Chem. A* **2025**, *129*, 3648-3662.
71. Ring, P.; Schuck, P. *The Nuclear Many-Body Problem*; Springer: New York, 1980, .
72. Depastas, T.; Souliotis, G. A.; Tzeli, D.; Xantheas, S. S. Many-Body Expansion for Light Nuclear Systems. *Phys. Rev. C* **2023**, *107*, 044004.
73. Blaschke, D.; Horiuchi, H.; Ring, P.; Röpke, G. The Nuclear Many-Body Problem Editorial Preface to the Topical Collection. *Eur. Phys. J. A* **2024**, *60*, 187.
74. Boys, S. F.; Bernardi, F. The Calculation of Small Molecular Interactions by the Differences of Separate Total Energies. Some Procedures with Reduced Errors (Reprinted from *Mol. Phys.* 19 (1970) 553-566). *Mol. Phys.* **1970**, *100*, 65-73.
75. Liu, B.; McLean, A. D. Accurate Calculation of the Attractive Interaction of Two Ground State Helium Atoms. *J. Chem. Phys.* **1973**, *59*, 4557-4558.
76. Jansen, H. B.; Ros, P. Non-Empirical Molecular Orbital Calculations on the Protonation of Carbon Monoxide. *Chem. Phys. Lett.* **1969**, *3*, 140-143.
77. Xantheas, S. S. On the Importance of the Fragment Relaxation Energy Terms in the Estimation of the Basis set Superposition Error Correction to the Intermolecular Interaction Energy. *J. Chem. Phys.* **1996**, *104*, 8821-8824.
78. Heitler, W.; Heitler, W. Quantum Chemistry: the Early Period. *Int. J. Quant. Chem.* **1967**, *1*, 13-36.
79. Miliordos, E.; Xantheas, S. S. Ground and Excited States of the $[Fe(H_2O)_6]^{2+}$ and $[Fe(H_2O)_6]^{3+}$ Clusters: Insight into the Electronic Structure of the $[Fe(H_2O)_6]^{2+}$ - $[Fe(H_2O)_6]^{3+}$ Complex. *J Chem Theory Comput.* **2015**, *11*, 1549-1563.
80. Tzeli, D.; Raugei, S.; Xantheas, S. S. Quantitative Account of the Bonding Properties of a Rubredoxin Model Complex $[Fe(SCH_3)_4]^q$, $q = -2, -1, +2, +3$. *J. Chem. Theory Comput.* **2021**, *17*, 6080-6091.
81. Xu, L. T.; Thompson, J. V. K.; Dunning, T. H. Spin-Coupled Generalized Valence Bond Description of Group 14 Species: The Carbon, Silicon and Germanium Hydrides, XH_n ($n=1-4$). *J. Phys. Chem. A* **2019**, *123*, 2401-2419.
82. Röpke, G.; Xu, C.; Zhou, B., et al. Alpha-Like Correlations in ^{20}Ne , Comparison of Quartetting Wave Function and THSR Approaches. *Eur. Phys. J. A* **2024**, *60* (4), 89.

83. Pastore, A.; Schuck, P.; Viñas, X. Generic Size Dependences of Pairing in Ultrasmall Systems: Electronic Nano-Devices and Atomic Nuclei. *Eur. Phys. J. A* **2023**, *59* (10), 241.
84. Bonasera, A.; Giuliani, G.; Zheng, H. *Prog. Part. Nuc. Phys.* **2014**, *76*, 116–164.
85. Kanada-Enyo, Y.; Kimura, M.; Ono, A. *Prog. Theor. Exp. Phys* **2012**, *2012* (1), 01A202.
86. Spiro, M.; Basdevant, J. L.; Rich, J. *Fundamentals in Nuclear Physics: From Nuclear Structure to Cosmology*; Springer: New York, 2005, .
87. Deev, V.; Collins, M. A. Approximate Ab Initio Energies by Systematic Molecular Fragmentation. *J. Chem. Phys.* **2005**, *122*, 154102.
88. Zhang, Da. W.; Zhang, J. Z. H. Molecular Fractionation with Conjugate Caps for Full Quantum Mechanical Calculation of Protein–Molecule Interaction Energy. *J. Chem. Phys.* **2003**, *119*, 3599–3605.
89. Heifetz, A.; Chudyk, E. I.; Gleave, L., et al. The Fragment Molecular Orbital Method Reveals New Insight into the Chemical Nature of GPCR–Ligand Interactions. *J. Chem. Inf. Model.* **2016**, *56* (1), 159–172.
90. Bowling, P. E.; Broderick, D. R.; Herbert, J. M. Fragment-Based Calculations of Enzymatic Thermochemistry Require Dielectric Boundary Conditions. *J. Phys. Chem. Lett.* **2023**, *14* (16), 3826–3834.